

NAVAL POSTGRADUATE SCHOOL Monterey, California



Modal Analysis of a GA Superconducting Magnet Subsystem for ALISS

by

M. Lee
Y. S. Shin

April 1997

Approved for public release; distribution is unlimited.

Prepared for: Naval Surface Warfare Center
Annapolis, MD 21402

THIS DOCUMENT CONTAINS

19970521 028

DISCLAIMER NOTICE



THIS DOCUMENT IS BEST QUALITY AVAILABLE. THE COPY FURNISHED TO DTIC CONTAINED A SIGNIFICANT NUMBER OF COLOR PAGES WHICH DO NOT REPRODUCE LEGIBLY ON BLACK AND WHITE MICROFICHE.

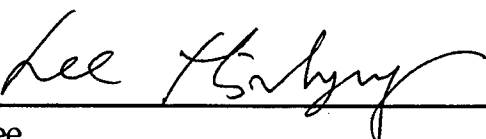
Naval Postgraduate School
Monterey, California

Real Admiral M. J. Evans
Superintendent

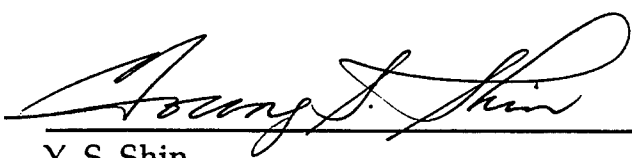
R. S. Elster
Provost

This report was prepared in conjunction with research conducted for Naval Surface Warfare Center, Annapolis, MD.

This report was prepared by:



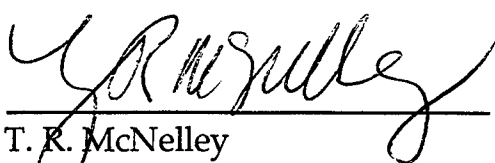
M. Lee
Research Assistant Professor of Mechanical Engineering



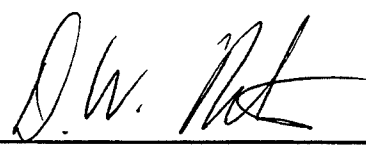
Y. S. Shin
Professor of Mechanical Engineering

Reviewed by:

Released by:



T. R. McNelley
Chairman
Dept. of Mechanical Engineering



D. W. Netzer
Dean of Research

REPORT DOCUMENTATION PAGE			Form Approved OMB No. 0704-0188	
Public reporting burden for this collection of information is estimated to average 1 hour per response, including the time for reviewing instructions, searching existing data sources, gathering and maintaining the data needed, and completing and reviewing the collection of information. Send comments regarding this burden estimate or any other aspect of this collection of information, including suggestions for reducing this burden to Washington Headquarters Services, Directorate for Information Operations and Reports, 1215 Jefferson Davis Highway, Suite 1204, Arlington, VA 22202-4302, and to the Office of Management and Budget, Paperwork Reduction Project (0704-0188), Washington, DC 20503.				
1. AGENCY USE ONLY (Leave Blank)		2. REPORT DATE 17 April, 1997		3. REPORT TYPE AND DATES COVERED FY1997
4. TITLE AND SUBTITLE MODAL ANALYSIS OF A GA SUPERCONDUCTING MAGNET SUBSYSTEM FOR ALISS			5. FUNDING NUMBERS N00167-96-WR-60497	
6. AUTHOR(S) M. Lee and Y. S. Shin				
7. PERFORMING ORGANIZATION NAME(S) AND ADDRESS(ES) Naval Postgraduate School Monterey, CA 93943-5000			8. PERFORMING ORGANIZATION REPORT NUMBER NPS-ME-97-004	
9. SPONSORING/MONITORING AGENCY NAME(S) AND ADDRESS(ES) Naval Surface Warfare Center Annapolis, MD			10. SPONSORING/MONITORING AGENCY REPORT NUMBER	
11. SUPPLEMENTARY NOTES The views expressed are those of the authors and do not reflect the official policy or position of DOD or US Government				
12a. DISTRIBUTION/AVAILABILITY STATEMENT Approved for public release: Distribution is unlimited			12b. DISTRIBUTION CODE	
13. ABSTRACT (Maximum 200 words) The modal analysis of a superconducting magnet subsystem designed by General Atomics (GA) has been performed to determine the natural frequencies and corresponding mode shapes. GA subsystem is a part of ALISS (Advanced Lightweight Influence Sweep System), which uses a superconducting magnet for magnetic mine sweeping. Any resonance condition must be avoided in an operational environment to ensure the no- quenching in the subsystem.				
14. SUBJECT TERMS ALISS, modal analysis, superconducting magnet sussystem			15. NUMBER OF PAGES 46	
			16. PRICE CODE	
17. SECURITY CLASSIFICATION OF REPORT Unclassified	18. SECURITY CLASSIFICATION OF THIS PAGE Unclassified	19. SECURITY CLASSIFICATION OF ABSTRACT Unclassified	20. LIMITATION OF ABSTRACT SAR	

ABSTRACT

The modal analysis of a superconducting magnet subsystem designed by General Atomics (GA) has been performed to determine the natural frequencies and corresponding mode shapes. GA subsystem is a part of ALISS (Advanced Lightweight Influence Sweep System), which uses a superconducting magnet for magnetic mine sweeping. Any resonance condition must be avoided in an operational environment to ensure the no-quenching in the subsystem.

TABLE OF CONTENTS

1. INTRODUCTION.	1
A. OVERVIEW.	1
B. RESEARCH OBJECTIVES	2
2. FINITE ELEMENT METHOD	3
3. FINITE ELEMENT MODELING	4
A. SOLID MODELING.	4
B. FINITE ELEMENT MODELING	8
4. NORMAL MODE ANALYSIS	14
5. DISCUSSIONS	29
APPENDIX A: MODE SHAPES OF ALISS	31
LIST OF REFERENCES	35
INITIAL DISTRIBUTION LIST	36

LIST OF FIGURES

Figure 1.	Cross Section of ALISS Magnetic Components.	6
Figure 2.	ALISS Module (a) with thermal shield, and (b) without thermal shield	7
Figure 3.	Finite Element Model of Magnetic ALISS Module	11
Figure 4.	Finite Element Model of Each Parts	12
Figure 5.	Finite Element Model of Each Parts	13
Figure 6.	Mode 1, 47.44 Hz, Axial and Lateral Translation. Coil.	16
Figure 7.	Mode 2, 47.44 Hz, Same as 1st Mode. Coil	17
Figure 8.	Mode 3, 62.97 Hz, Breeding Mode. Coil	18
Figure 9.	Mode 3, 62.97 Hz, Breeding Mode. Outer S Glass.	19
Figure 10.	Mode 4, 64.54 Hz, Bending Mode. Coil.	20
Figure 11.	Mode 5, 64.58 Hz, Same as 4th Mode. Outer S Glass	21
Figure 12.	Mode 6, 75.50 Hz, Rocking & Bending Mode. Coil.	22
Figure 13.	Mode 7, 75.50 Hz, Same as 6th Mode. Outer S Glass	23
Figure 14.	Mode 8, 86.15 Hz, Axial Translation. Coil	24
Figure 15.	Mode 8, 75.50 Hz, Axial Translation. Outer S Glass	25
Figure 16.	Mode 9, 101.96 Hz, Twisting Mode. Titanium ring (10K)	26
Figure 17.	Mode 9, 101.96 Hz, Twisting Mode. Coil.	27
Figure 18.	Mode 10, 101.97 Hz, Combined Bending Mode. Coil	28

LIST OF TABLES

Table I	Physical Properties of Shell Element	10
Table II	List of Material Properties	10
Table III	Natural Frequencies	14

1. INTRODUCTION

A. OVERVIEW

There are two broad classifications of mines: contact mines and influence mines. [Ref. 1] Contact mines utilize the simplest technology and detonate only after coming into direct physical contact with targets. Influence mines detonate when they detect more characteristic ship or submarine signatures within range of the mines. The signatures are generated by acoustic noise, magnetic field variations, and hydrostatic pressure changes.

Mine hunting is the localization, identification, and neutralization of individual mines. There are two mine countermeasures (MCM) presently in use by the U.S. Navy for mine hunting and mine sweeping; a Current injection system and permanent magnetic system. [Ref. 2] The Current injection system creates magnetic signatures in sea water by passing a current through two separate electrodes. The permanent magnetic system composed of large steel pipe is towed by helicopters for shallow water sweeping. It is approximately a 30 foot length of 10 inch diameter steel pipe filled with Styrofoam and magnetized. Currently, there exists no capability in the U.S. Navy to sweep magnetic mines at speeds above 25 knots or in water shallower than 12 foot.

ALISS is an Advanced Technology Demonstration (ATD) to show how modules of relatively new, undeveloped technologies may be combined to provide the U.S. Navy with the capability to perform high-speed, shallow water mine countermeasures. [Ref. 3] There are three main elements to the magnetic sweeping module; a conductivity cooled superconducting magnet, a refrigeration system (cryocooler), and a cryostat. In this work, the vibration analysis is focused on the superconducting magnet and cryostat.

B. RESEARCH OBJECTIVES

The use of a superconducting mine countermeasures system such as ALISS provides some advantages over present current injection and permanent magnet systems. Because of the small size and modularity of ALISS, it can be deployed onboard such vehicles as the Navy's LCAC (Landing Craft Air Cushing) or the Army's LACV (Landing Air Cushing Vehicle) classes of air-cushion landing craft at high-speed. Since ALISS is designed to operate while mounted to a moving vehicle, the vibration created in the system must be properly isolated within the system to ensure proper operation of the superconductor. Furthermore, ALISS is subjected to shock loads from underwater explosions (UNDEX). In this shock environment, it is possible for the superconducting magnet to become resistive (quenching). It is operationally unacceptable for the ALISS system to remain idle.

The purpose of this study is to build a finite element model of a candidate module developed by the General Atomics (GA) [Ref. 4] and perform modal analysis of the model.

2. FINITE ELEMENT METHOD

The finite element method is a numerical procedure for approximating the solution to many complex problems encountered in engineering. An approximate solution to the theoretical behavior of complex structures are obtained at a finite set of points in the model. The accuracy of a finite element solution depends on the way the finite element model is generated. That is, it depends on the number and type of elements used in the model.

Free vibration analysis is a method for predicting the undamped vibration characteristics of a structure. This vibration takes place in the absence of external excitation. The equation of motion of a discrete system is written in matrix form as,

$$[M]\{\ddot{q}\} + [K]\{q\} = \{0\}, \quad (1)$$

where, $[M]$ is the structural mass matrix, $\{\ddot{q}\}$ is the nodal acceleration vector, $[K]$ is the structural stiffness matrix and $\{q\}$ is the nodal displacement vector. Equation (1) is a system of coupled differential equations with n -independent unknowns, where n is the total number of degrees-of-freedom in the structure. By assuming a solution of the form as,

$$\{q\} = C\{\phi\}e^{j\omega t}, \quad (2)$$

an n -th order homogeneous eigenvalue problem is generated as,

$$[-\omega^2[M] + [K]]Ce^{j\omega t} = 0, \quad (3)$$

where, C is a constant and $\{\phi\}$ is a spatial vector. The non-trivial solution to Equation (3) is,

$$\det[-\omega^2[M] + [K]] = 0 \quad (4)$$

This is the characteristic equation of the system. The roots of this equation are the eigenvalues, $\lambda_i = \omega_i^2$, where each ω_i is a natural frequency of vibration.

For each natural frequency, there is a corresponding eigenvector $\{\phi\}$ that is the mode shape associated with that frequency. Thus, the solution to the free vibration is n eigenpairs, ω_n and $\{\phi^n\}$.

3. FINITE ELEMENT MODELING

The finite element (FE) model of the GA subsystem was built using *MSC/PATRAN* 6 code. The first step in finite element analysis was to build a solid model using the fabrication drawings provided by the manufacturer. Using the solid model as a geometric reference, a finite element model was built by manually creating nodes and elements. Certain features of the solid model such as bolt holes, scarf joints, and second stage sleeve were not transferred to the finite element model in order not to introduce large number of elements. Once a complete finite element model of the ALISS module was generated, physical and material properties of the various parts were then defined and a boundary condition was applied to the model. The modal analysis was carried out using *MSC/NASTRAN* [Ref. 5] code.

A. SOLID MODELING

This section provides a description of various parts modeled in the finite element analysis. The major components in cross section through cryostat are displayed in Figure 1. On the basis of structural design optimization determining that the lightest weight is achieved if the cylinders are smaller diameter than the magnetic coil, the structure is designed so it interfaces with the coil on its inside diameter. Innermost is the superconducting magnetic coil which contains NbTi conductor stabilized in

copper. The copper provides both mechanical and thermal stability to the superconductor.

Surrounding the coil is an aluminum overwrap and bobbin which provide for thermal conduction and support of the magnet. Since the overwrap is press-fit onto the coil, no slip is specified. Moving outward, the outer S-Glass cylinder which is attached to the bobbin circumferentially is connected to a titanium ring (10K). A middle E-Glass cylinder connects the titanium ring (10K) to a large titanium ring (40K). A outer shell of the aluminum thermal shield is connected to the titanium ring (40K). A inner E-Glass cylinder is made of the same material as the middle E-Glass cylinder and has similar construction. The inner E-Glass cylinder on the right side is connected to a vacuum vessel mount ring.

The parts previously described were generated in the modeling task by picking a basic shape from a catalog of primitives. Most of the primitives used were cylinders and rings. The parts that were modeled for this analysis were; overwrap, the magnetic coil, bobbin, outer S-Glass, titanium ring, middle E-Glass, thermal shield, and inner E-Glass. Figure. 2 is a solid representation of the finite element model.

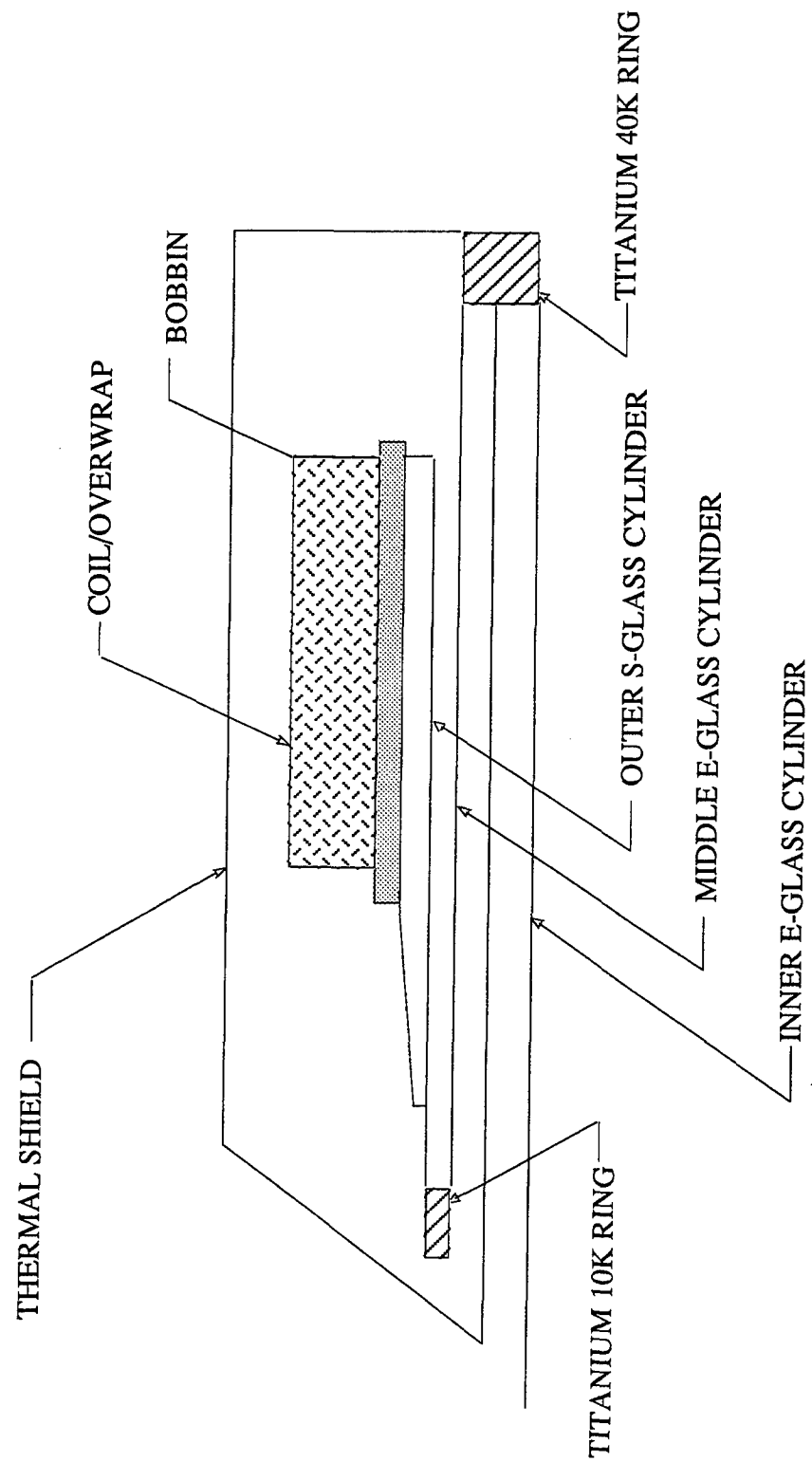
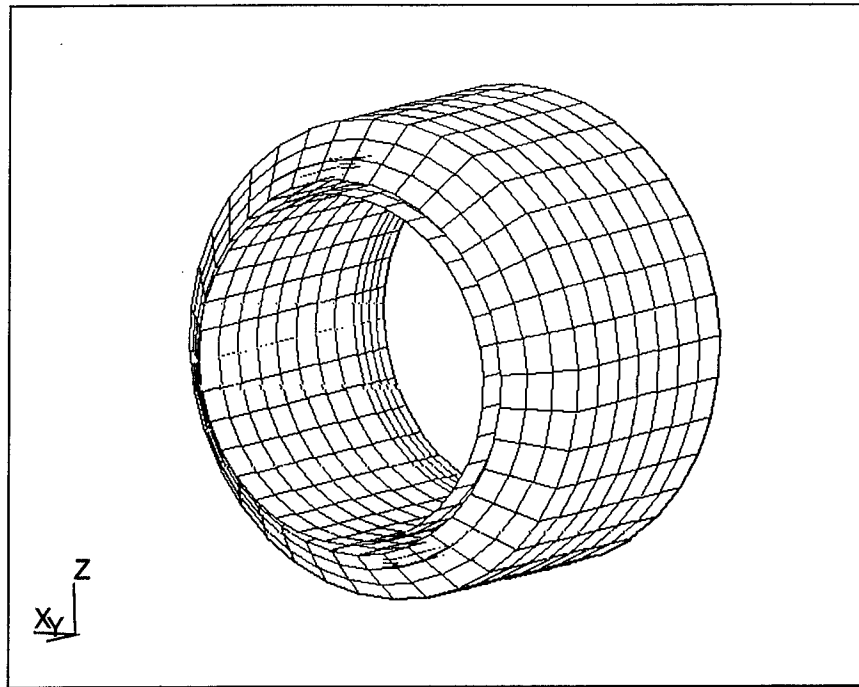
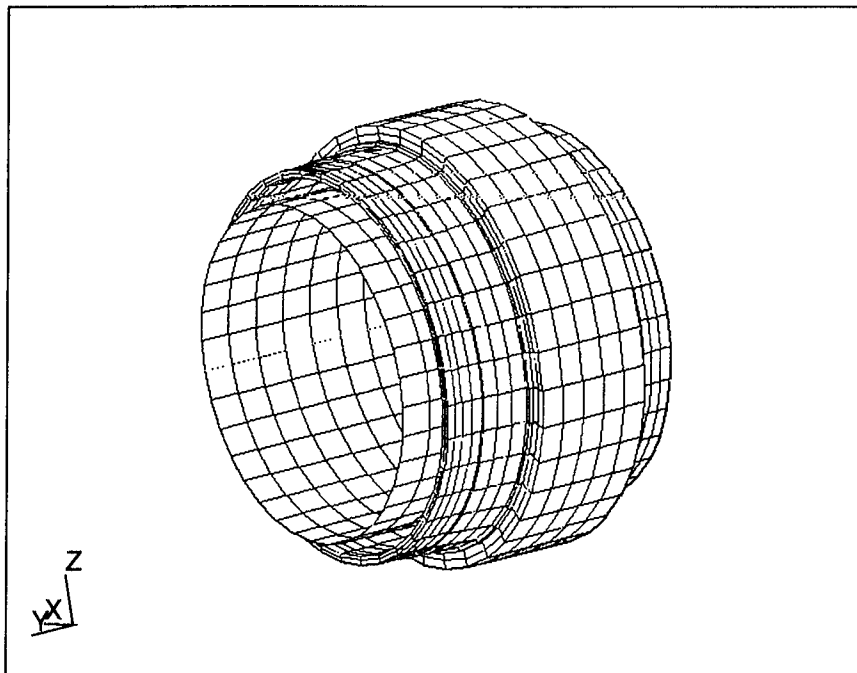


Figure 1. Cross Section of ALISS Magnetic Components [Ref. 4].



(a)



(b)

Figure 2. ALISS Module (a) with thermal shield, (b) without thermal shield.

B. FINITE ELEMENT MODELING

A certain idealization had been made to keep the mathematical model as small as possible with minimum impact on the solution accuracy. Hence, small features were suppressed when transferring geometric information from the solid model to the finite element model. Once each part was discretized individually, the various finite element representations of the parts were appended to each other to make the entire assembly. Figure 3 displays the finite elements of GA subsystem model.

The total number of nodes in the finite element model is 4958. There are several types of elements to choose when making a finite element model. The proper choice depends on the geometry to be generated. Most elements were also manually generated by specifying the types of element and the node points belongs to them. Two types of elements were used in the current model of the GA subsystem; thin shell elements and solid elements. Thin shell elements were used to model structures that are thin compared to their length and width. Quadrilateral shell elements defined by four nodes were used to represent the inner E Glass cylinder, middle E Glass cylinder, and thermal shield. Solid elements are used to represent structures whose thickness is of the same order as their other dimensions. Brick elements defined by eight nodes were used to represent titanium rings, outer S Glass cylinder, bobbin, overwrap, and the magnetic coil. Actually, titanium rings are composed of solid elements for the ring section and thin shell elements for the cylinder section. The total number of elements in the model is 2700. Since most of the parts are cylinders, it is more realistic to look at each part individually. The finite elements of each parts modeled are displayed in Figure 4 and Figure 5.

Once the finite elements are generated, identification of duplicate nodes, duplicate elements, and missing elements must be conducted in order to find errors that may have occurred during the mesh generation. If the model is properly constructed, the free edge will show the model boundaries. If there exist missing elements or nodes, the highlighted line will indicate either hole or a crack in the model.

After the finite element model was generated, the physical and material properties of each elements were specified. Table I provides a list of the element thickness of the thin shell elements. Material properties must be also specified for each part of the model. The titanium ring, thermal shield, and bobbin are isotropic: that is, the material properties are directional. Table II lists the properties of the various materials used in the finite element model. Since titanium rings are represented as having rectangular cross section, there exists a difference between the actual mass and modeled mass. To take this into account, the density of the titanium is slightly reduced as shown in Table II.

Finally, boundary conditions were applied to the finite element model to determine the normal modes of vibration. The zero displacement restraint is specified along the edge of the inner E Glass cylinder which is connected to the vacuum vessel mounting ring. For a transient analysis, this boundary condition should be replaced with a excitation restraint.

Table I Physical Properties of Shell Element

Part	Material	Thickness (inch)
Inner E Glass Cylinder	Composite	0.43
Middle E Glass Cylinder	Composite	0.4
Thermal Shield	Aluminum	0.145

Table II List of Material Properties

Name	E (radial)	E (hoop) psi	E (axial)	Density lb/cu in	Poisson's Ratio
Inner E Glass Cylinder	2.0E+6	2.69E+6	3.47E+6	0.067	0.3
Titanium Ring	1.8E+7	1.8E+7	1.8E+7	0.13	0.3
Thermal Shield	1.1E+7	1.1E+7	1.1E+7	0.098	0.3
Middle E-Glass Cylinder	3.0E+6	4.19E+6	4.88E+6	0.067	0.23
Outer S-Glass Cylinder	3.0E+6	6.63E+6	3.0E+6	0.067	0.23
Bobbin	1.1E+7	1.1E+7	1.1E+7	0.098	0.3
Coil/Overwrap	3.52E+6	1.3E+7	5.32E+6	0.19	0.3

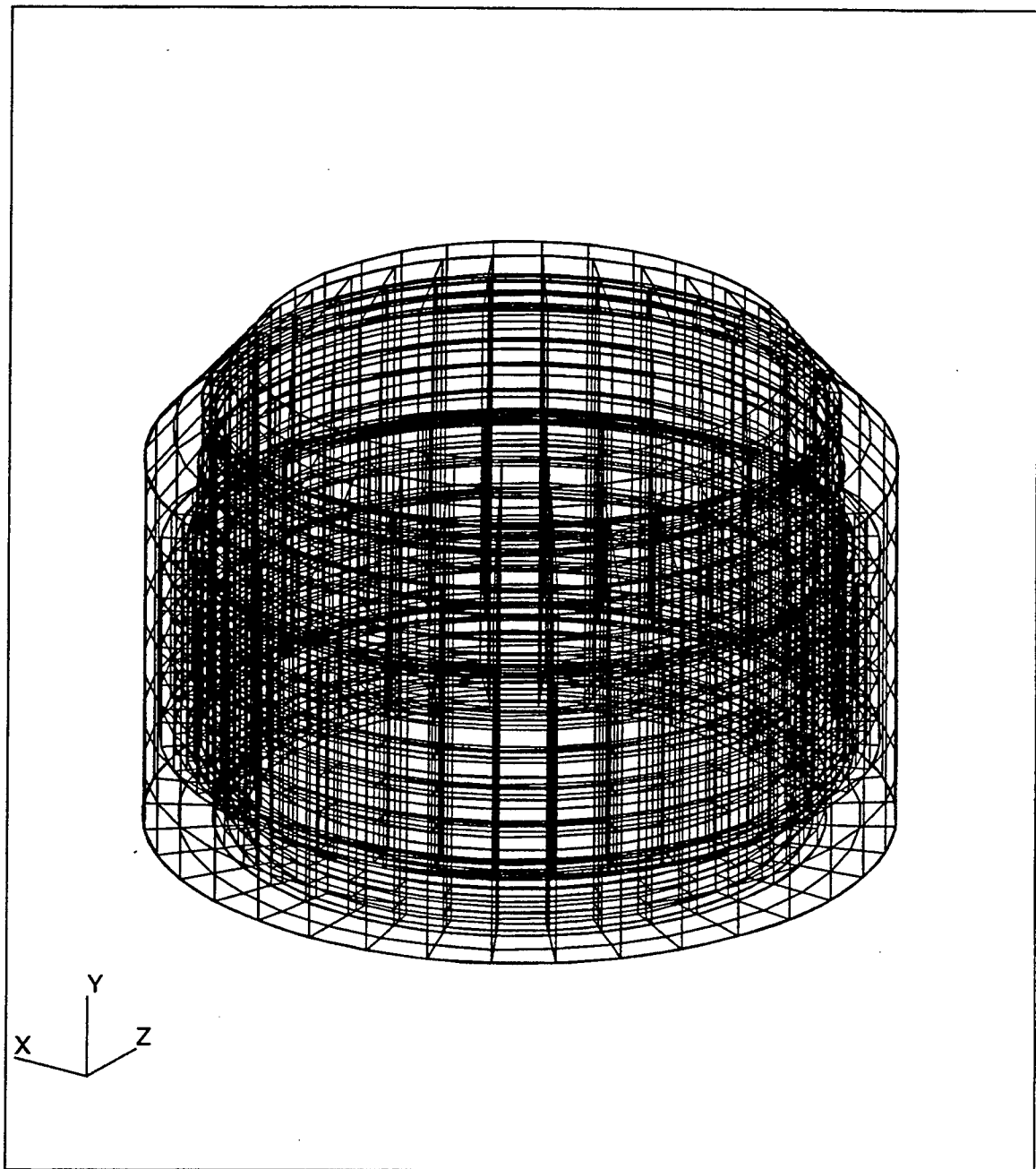


Figure 3. Finite Element Model of Magnetic ALISS Module.

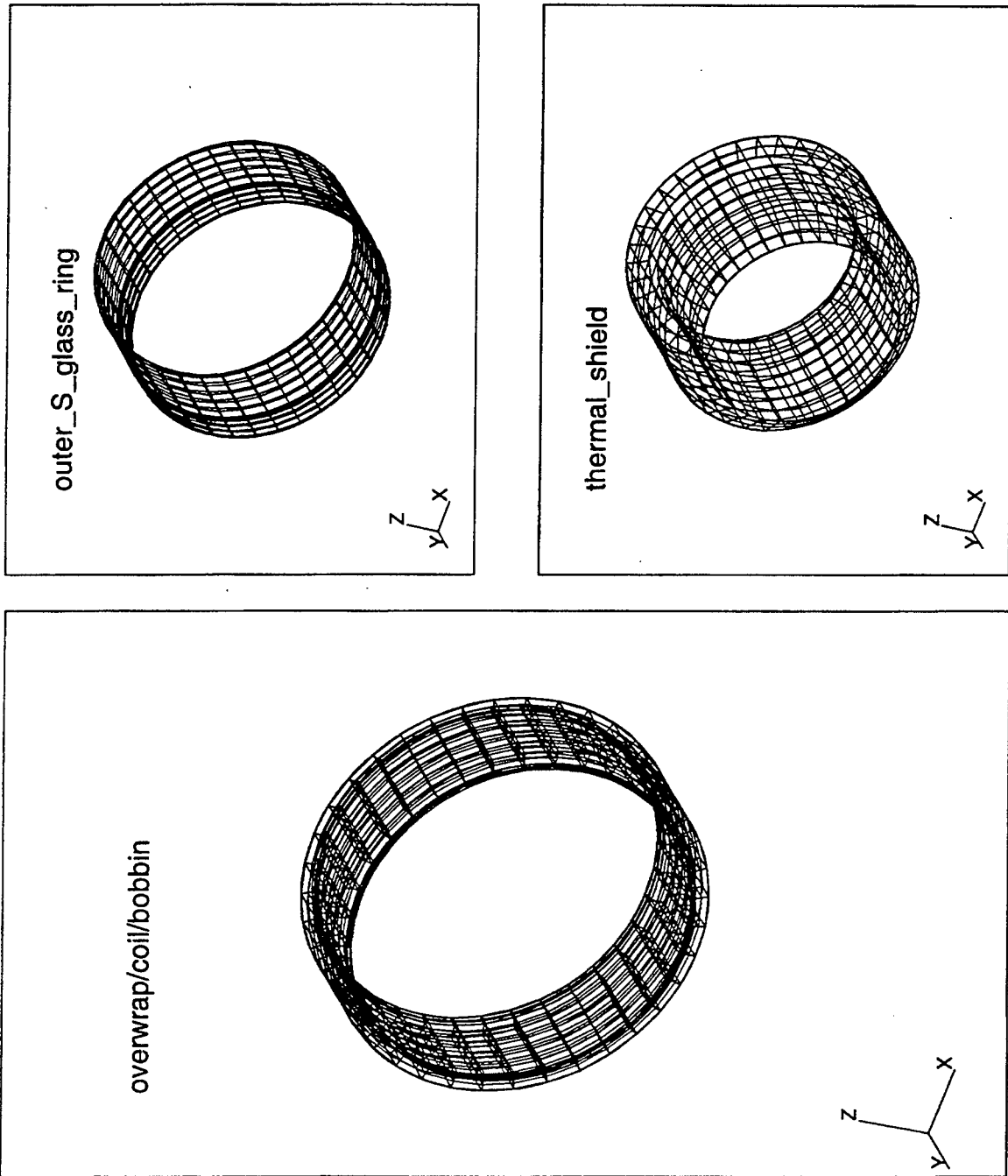


Figure 4. Finite Element Model of Each Parts.

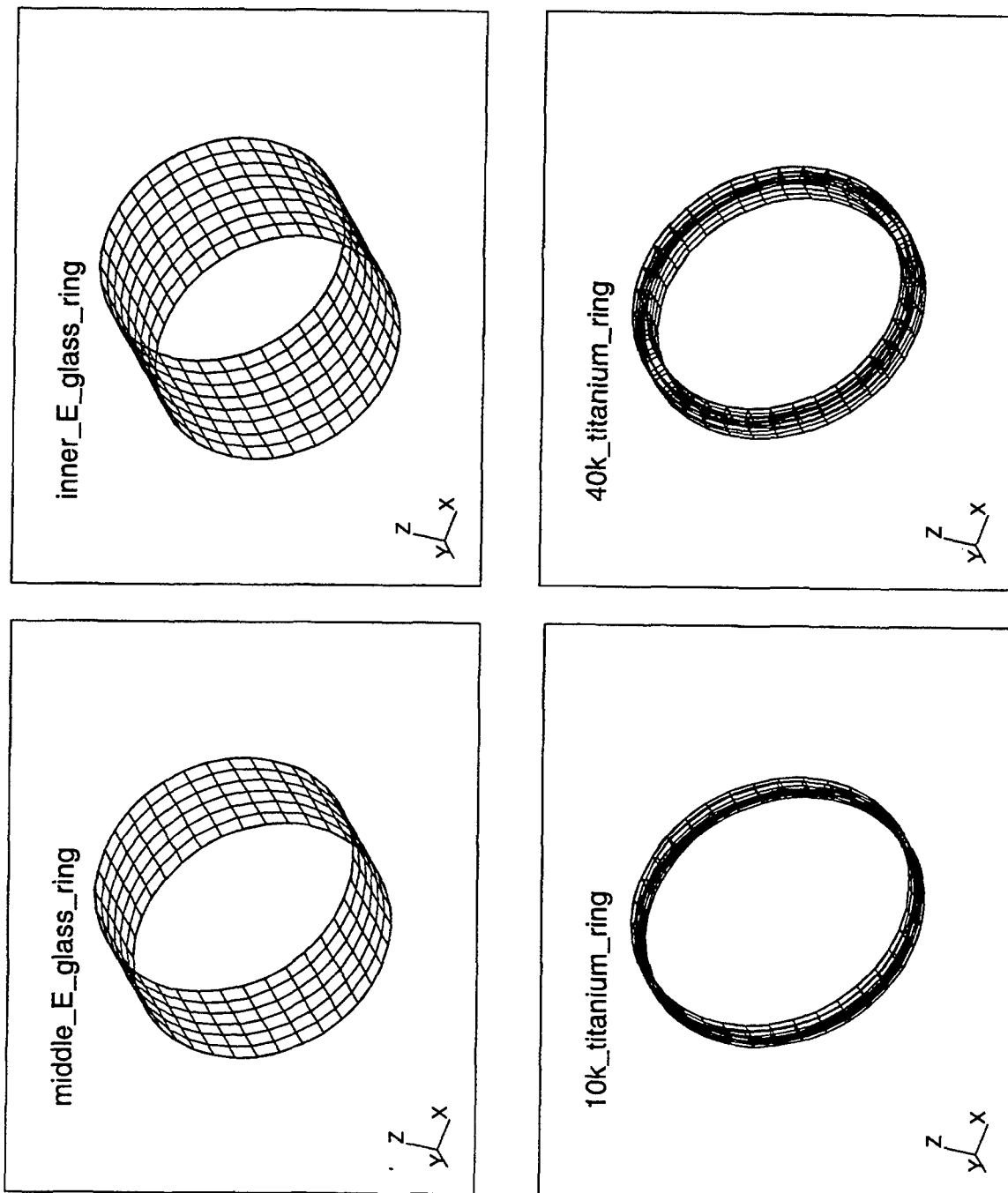


Figure 5. Finite Element Model of Each Parts.

4. NORMAL MODE ANALYSIS

The normal modes of vibration of the model were solved using *MSC/NASTRAN* finite element structural code. The solutions are the system undamped natural frequencies and the mode shapes.

The first 10 modes of the model were obtained and the natural frequencies are provided in Table III. Due to the connectivity of each part in the finite element model, resonant frequencies of one component have effects on the other parts to some degrees. In the following discussion, thus, the mode shapes are depicted by describing the motions of the parts that exhibit the greatest deformation value from the eigenvector. The deformation shown in the figures are not to scale with the parts.

Table III. Natural Frequencies.

Mode Natural Frequency (Hz)	
1	47.44
2	47.44
3	62.97
4	64.54
5	64.58
6	75.50
7	75.50
8	86.15
9	101.96
10	101.97

Only the modes that have significant deformations of a part are described here. Appendix A gives complete characteristics of the first 10 modes of this model.

The major participant in Mode 1 at 47.44 Hz is the magnetic coil. Figure 4 shows this mode. The magnetic coil translates axially and laterally. There is

also a slight rocking motion of the coil. Mode 2 occurs at the same frequency and has the same shapes as Mode 1, which is also displayed in Figure 7.

Mode 3, which occurs at 62.97 Hz, is characterized by coil and outer S Glass cylinder deforming in a breathing fashion. The maximum deformations of the coil and outer S Glass cylinder caused by this mode are shown in Figure 8 and Figure 9, respectively.

The primary motion of Modes 4 (64.54 Hz) and 5 (64.58 Hz) are bending of the coil and outer S Glass cylinder. The maximum deformations of the coil and outer S Glass cylinder caused by this mode are shown in Figure 10 and Figure 11, respectively.

The natural frequency of Mode 6 is 75.50 Hz. This mode is identified by the rocking and bending motions in coil and outer S Glass cylinder. The maximum deformations of the coil caused by this mode are shown in Figure 12. Mode 7 vibrates at nearly the same frequency and the deformation of the outer S Glass cylinder caused by this mode are displayed in Figure 13.

The primary participant in Mode 8, which occurs in 86.15 Hz are the coil and outer S Glass cylinder. The motion of these parts is axial translational motion. The deformations of the coil and outer S Glass cylinder caused by this mode are shown in Figure 14 and Figure 15, respectively.

The major parts in Mode 9 at 101.96 Hz are Titanium Ring (10K), middle E Glass cylinder, outer E Glass cylinder, and coil. They exhibit the twisting motions. The deformations of the Titanium Ring and coil caused by this mode are shown in Figure 16 and Figure 17, respectively. Figure 18 shows the combined bending motion of the coil occurring at 101.97 Hz.

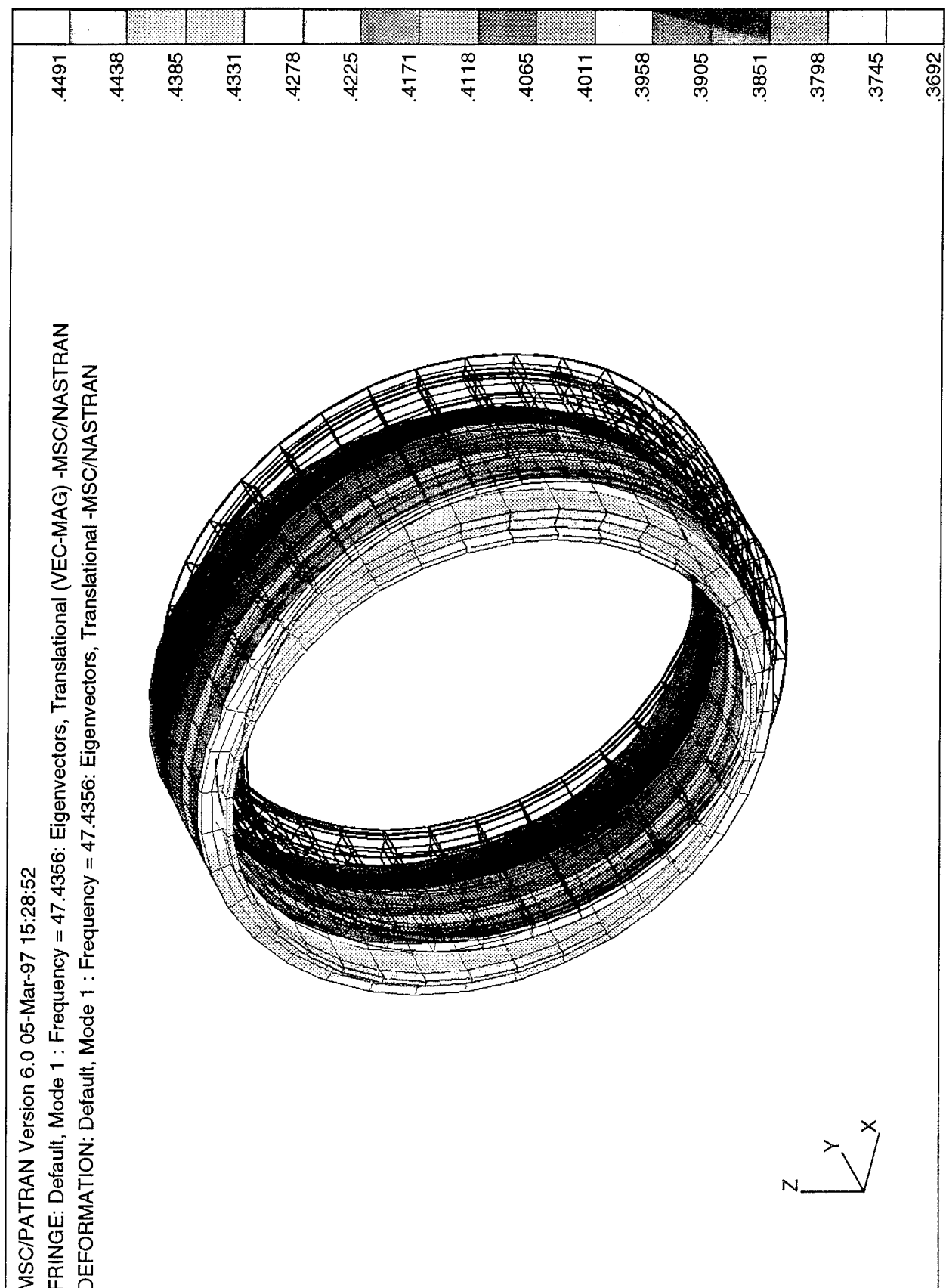


Figure 6. Mode 1, 47.44 Hz, Axial and Lateral Translation. Coil.

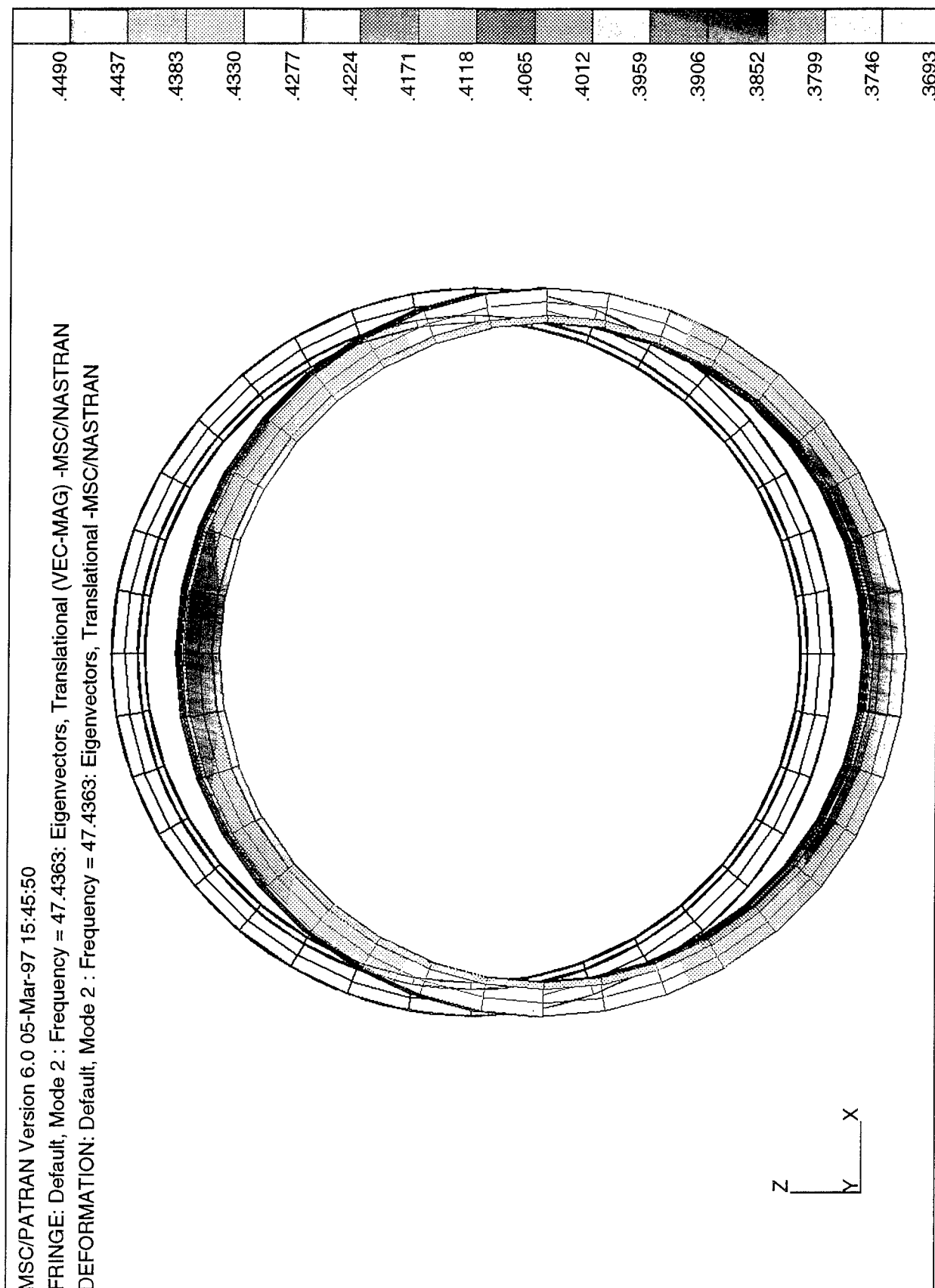


Figure 7. Mode 2, 47.44 Hz, Same as 1st Mode. Coil.

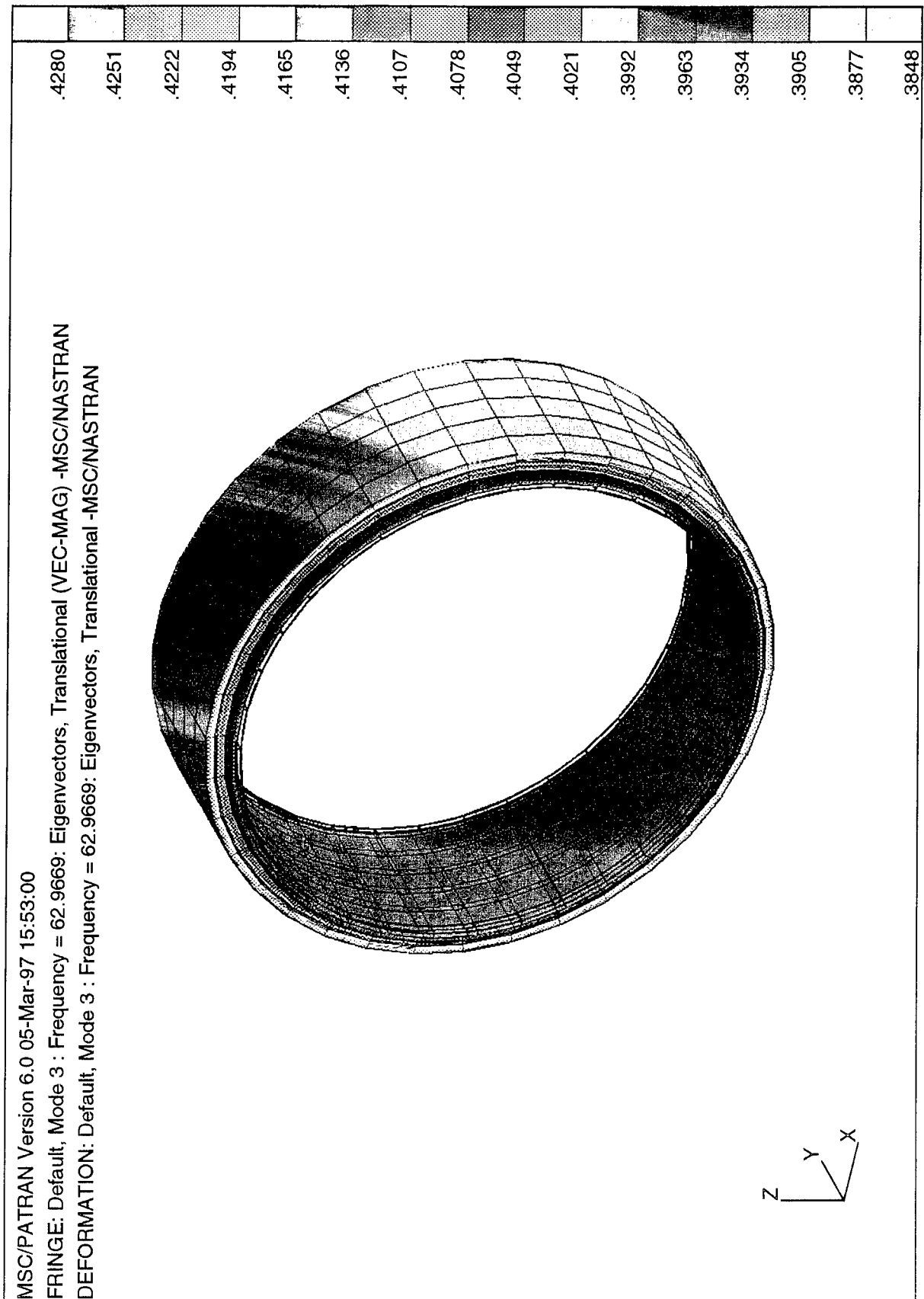


Figure 8. Mode 3, 62.97 Hz, Breeding Mode. Coil.

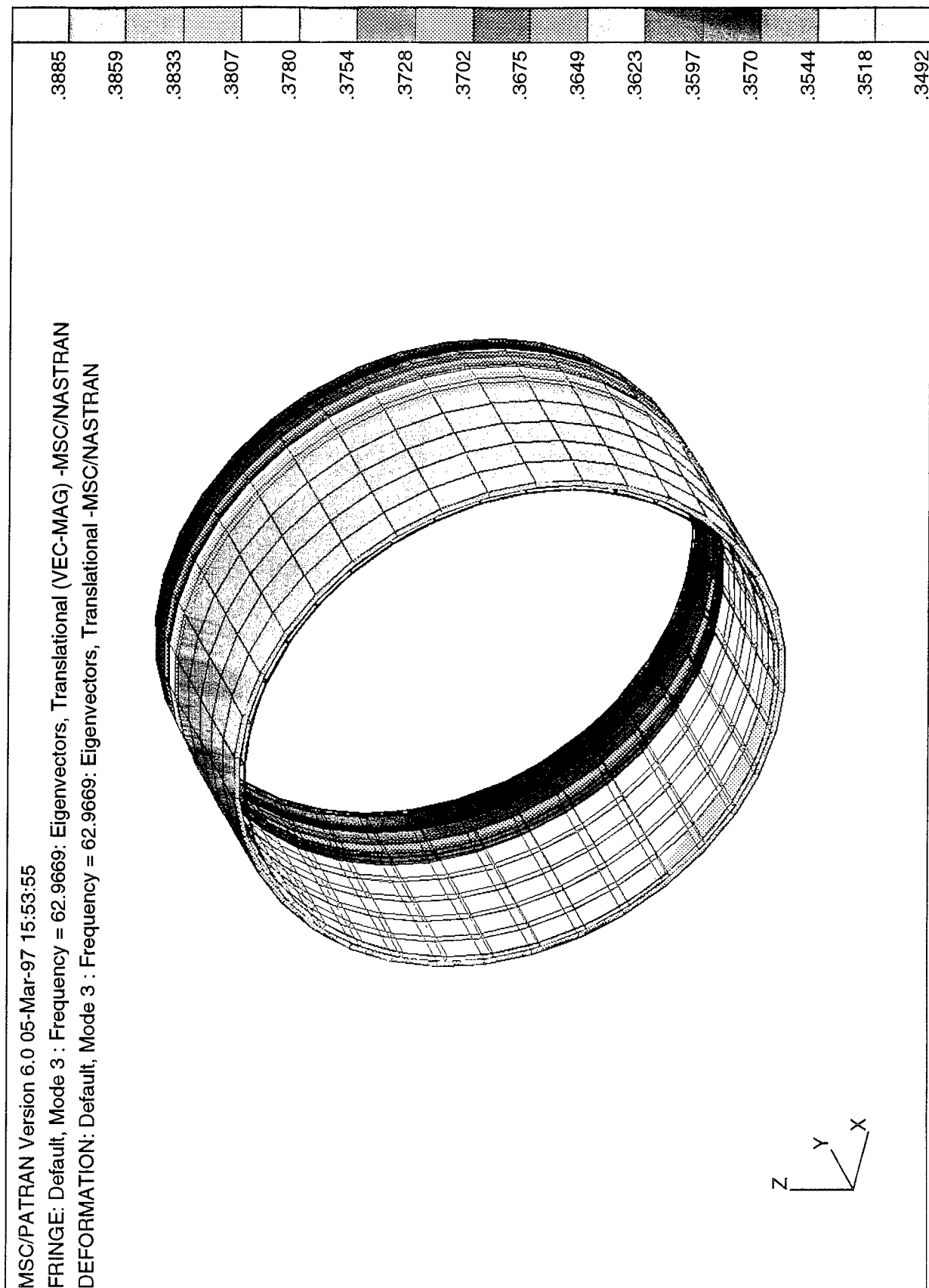


Figure 9. Mode 3, 62.97 Hz, Breeding Mode. Outer S Glass.

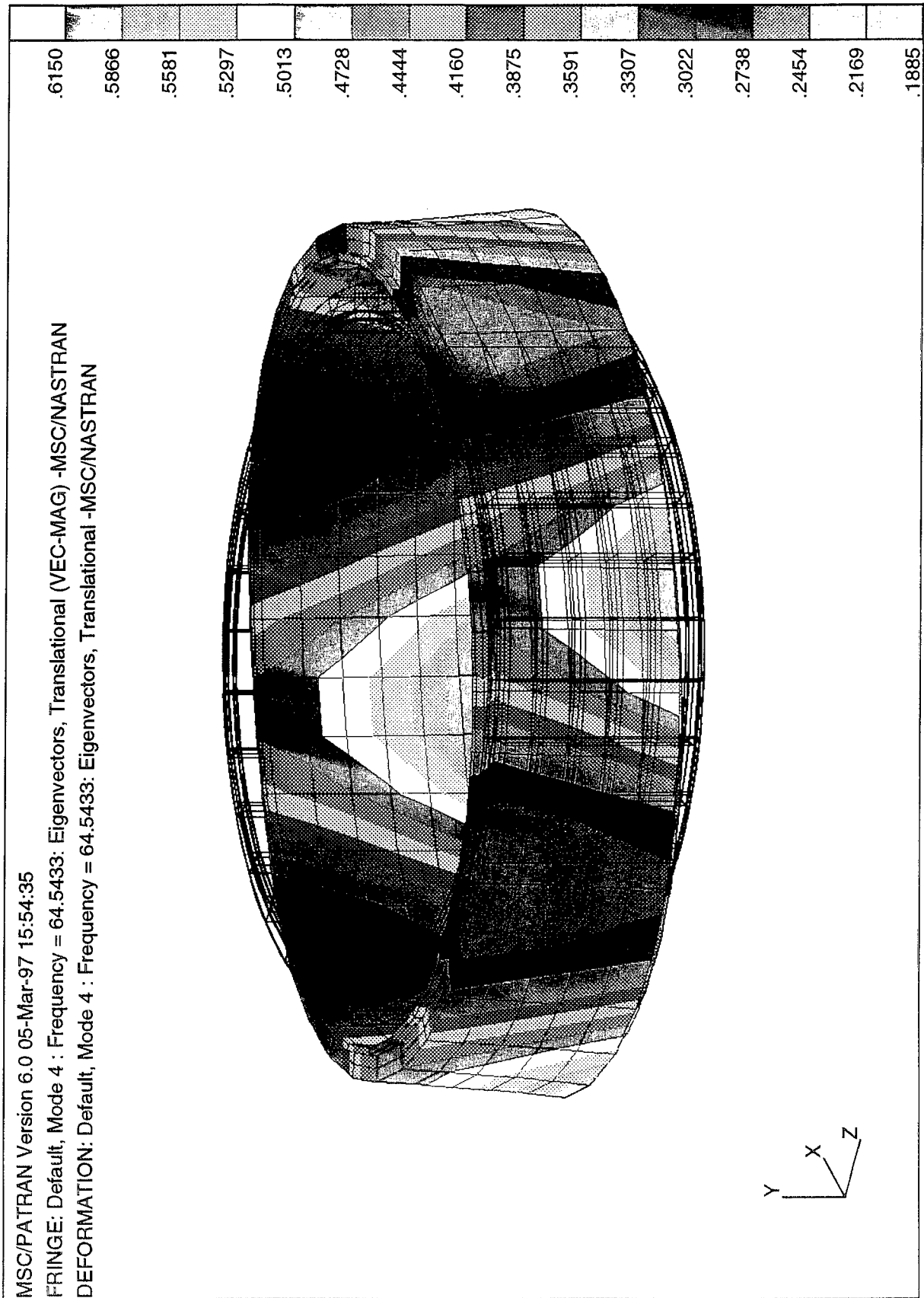


Figure 10. Mode 4, 64.54 Hz, Bending Mode. Coil.

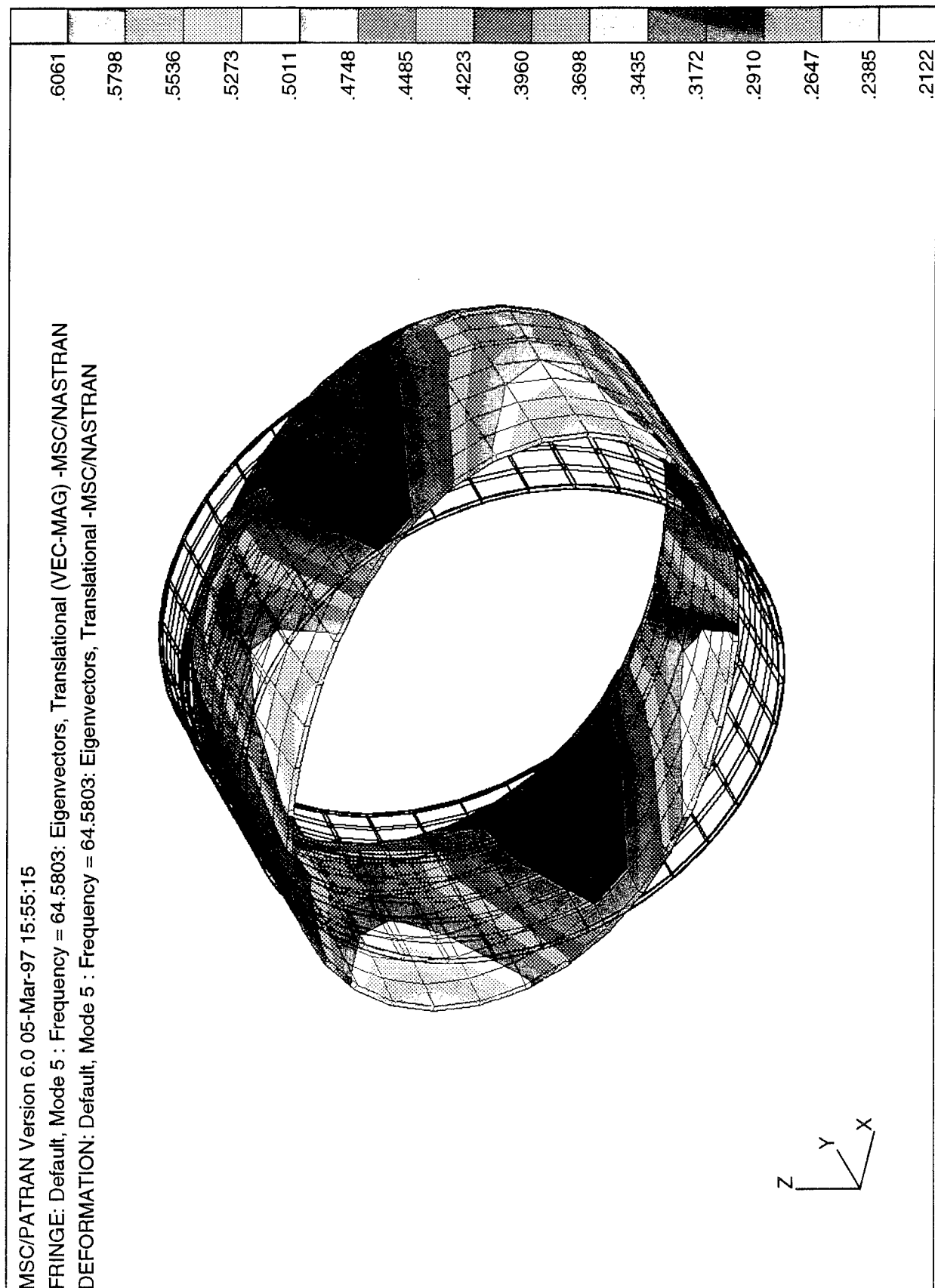


Figure 11. Mode 5, 64.58 Hz, Same as 4th Mode. Outer S Glass.

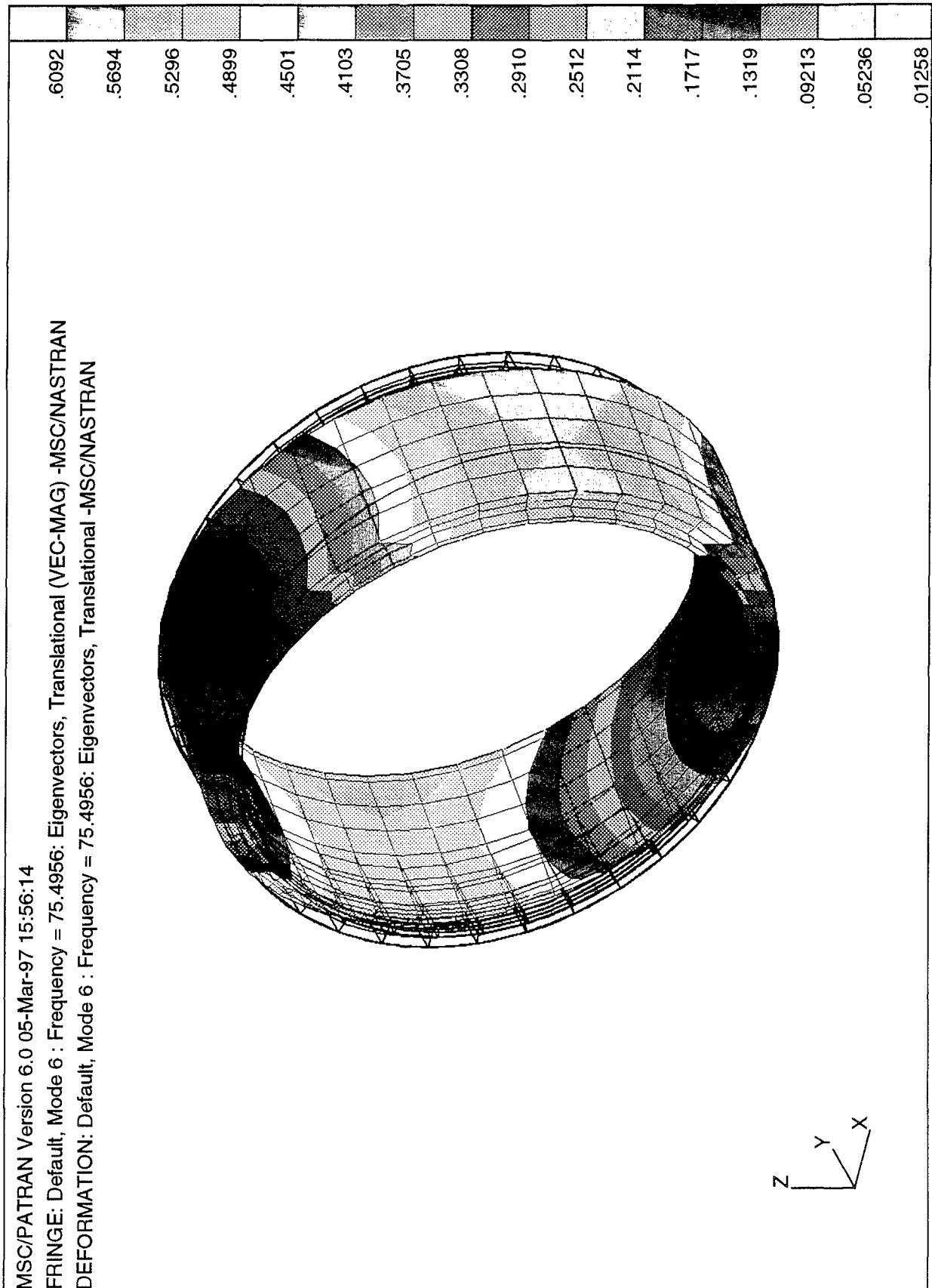


Figure 12. Mode 6, 75.50 Hz, Rocking & Bending Mode. Coil.

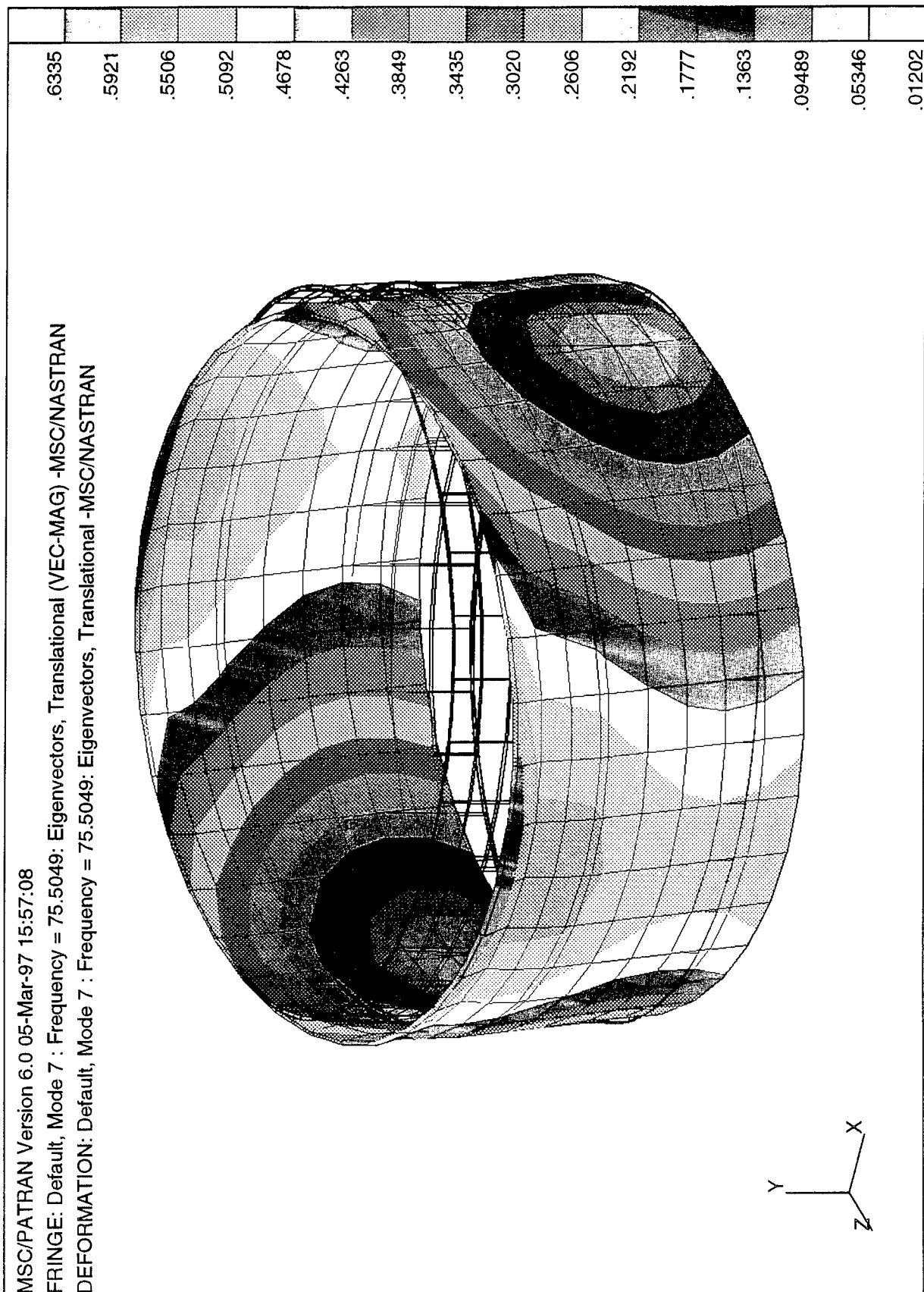


Figure 13. Mode 7, 75.50 Hz, Same as 6th Mode. Outer S Glass.

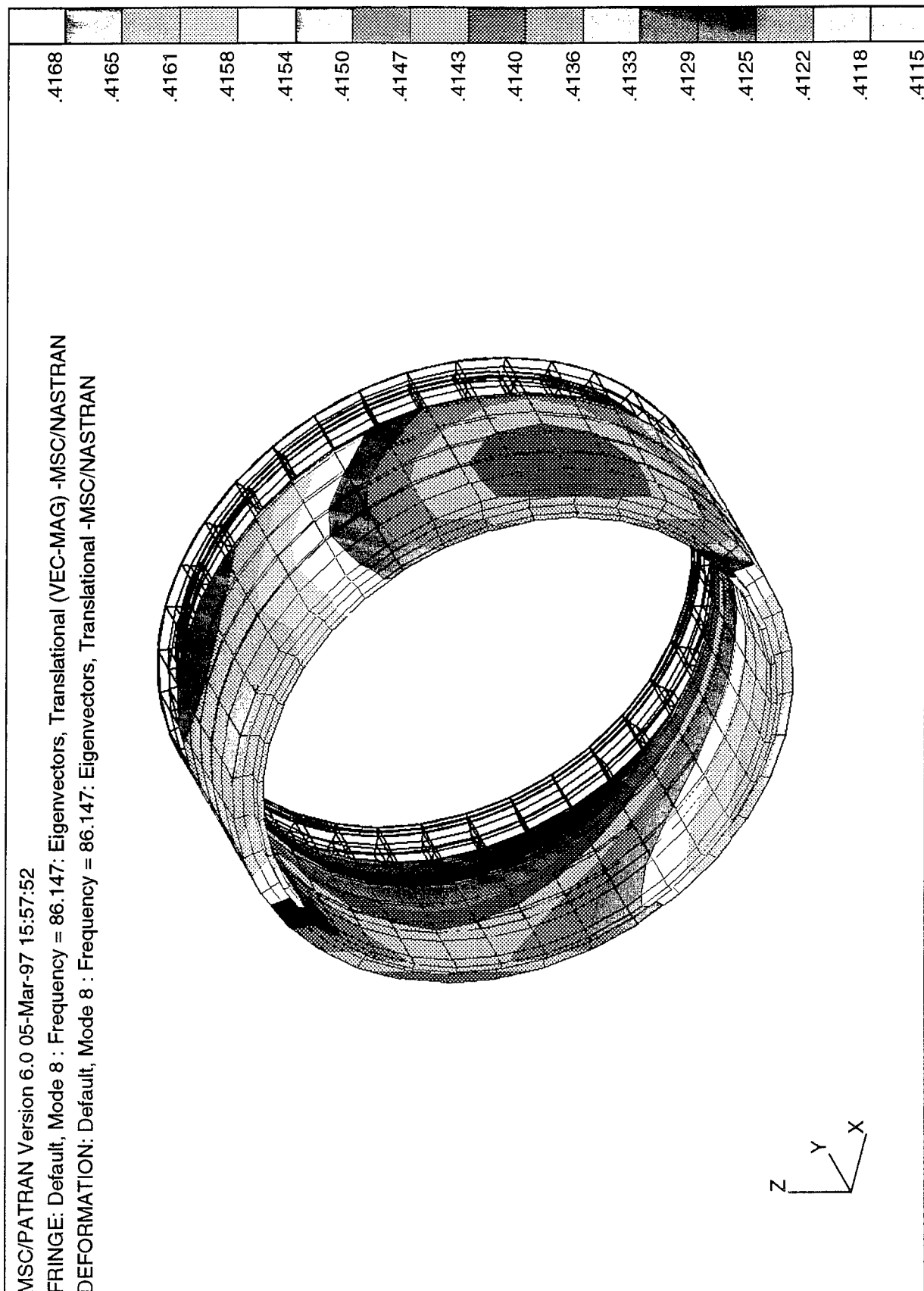


Figure 14. Mode 8, 86.15 Hz, Axial Translation. Coil.

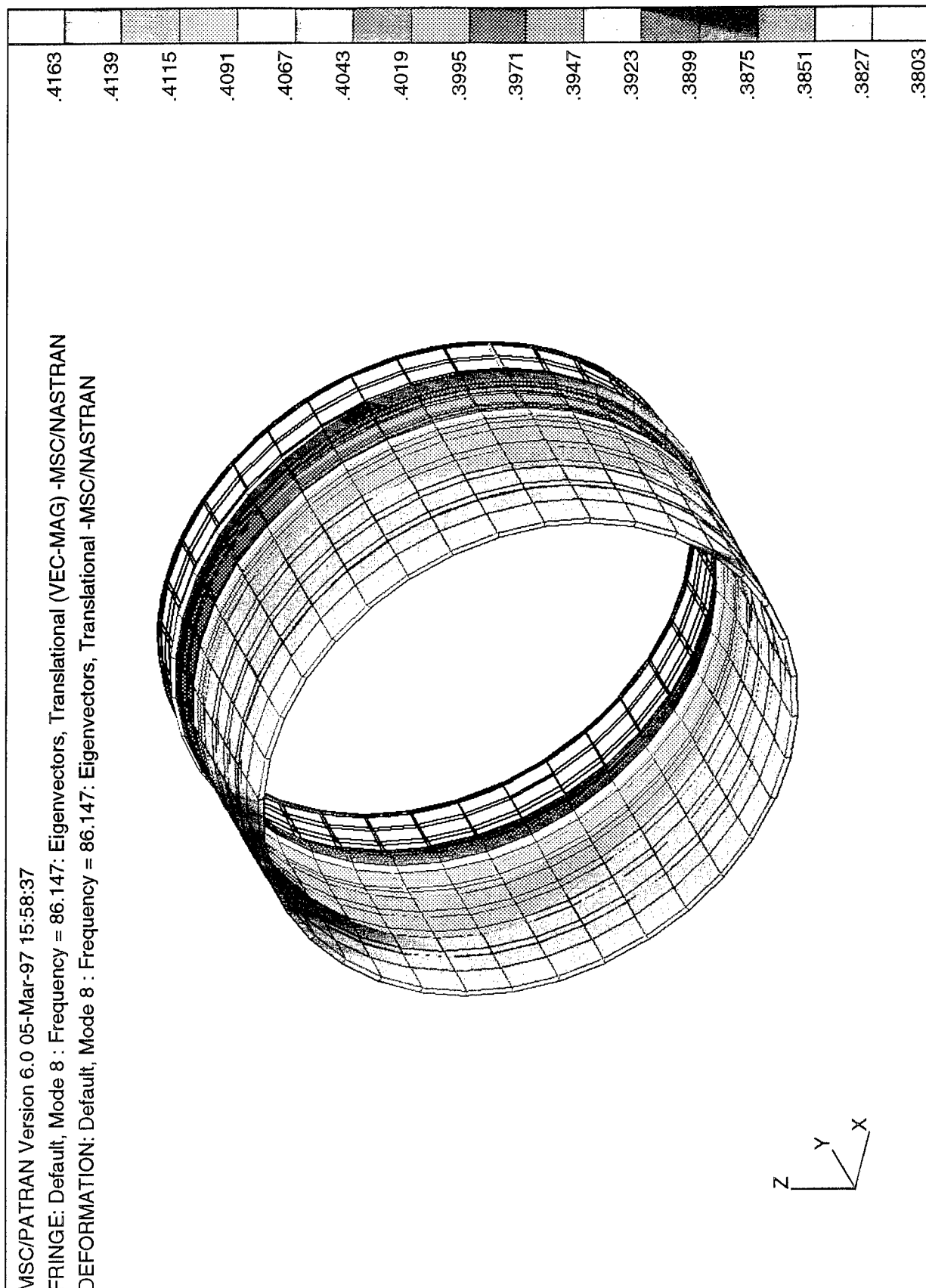


Figure 15. Mode 8, 75.50 Hz, Axial Translation. Outer S Glass.

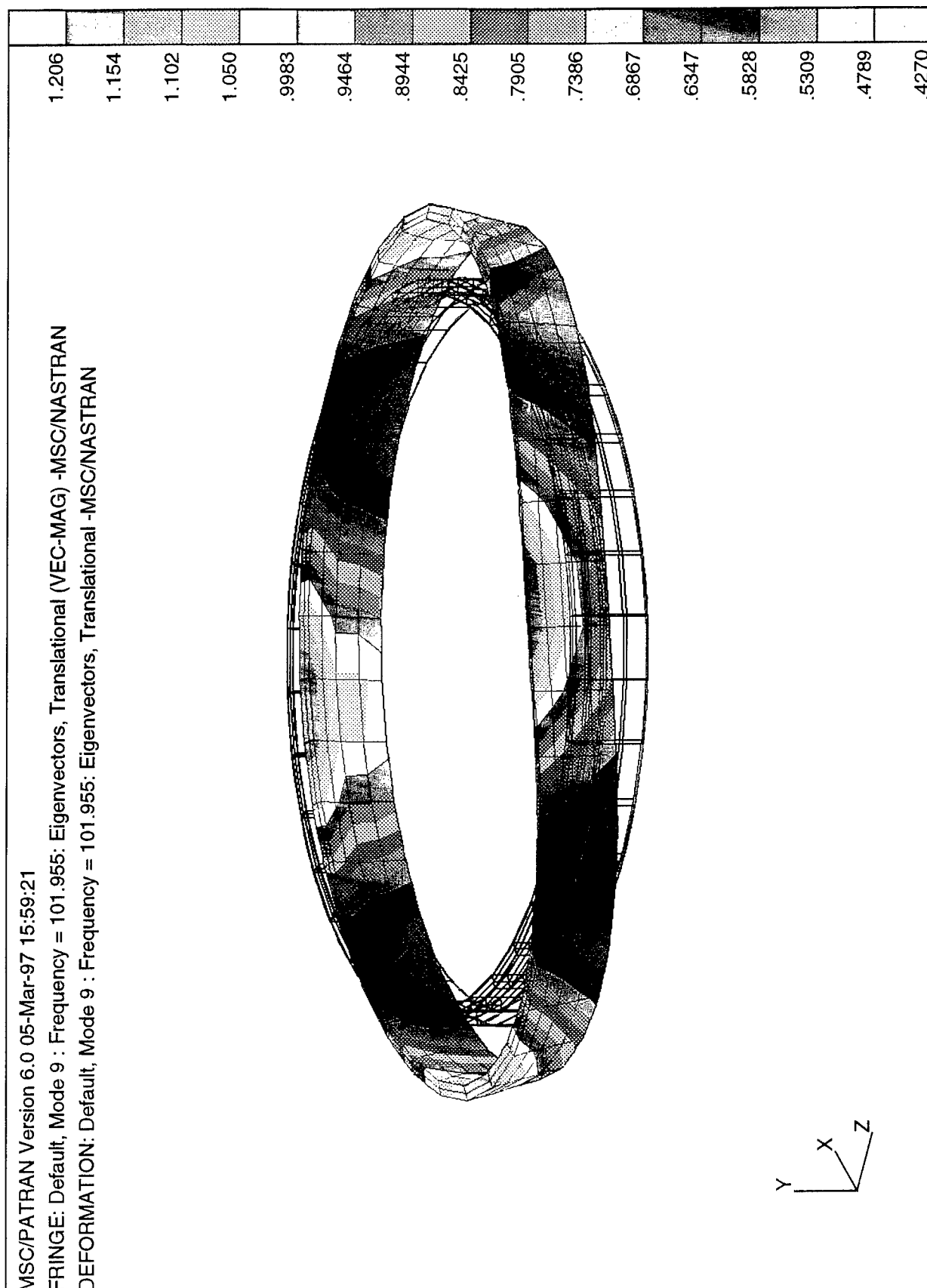


Figure 16. Mode 9, 101.96 Hz, Twisting Mode. Titanium ring (10K).

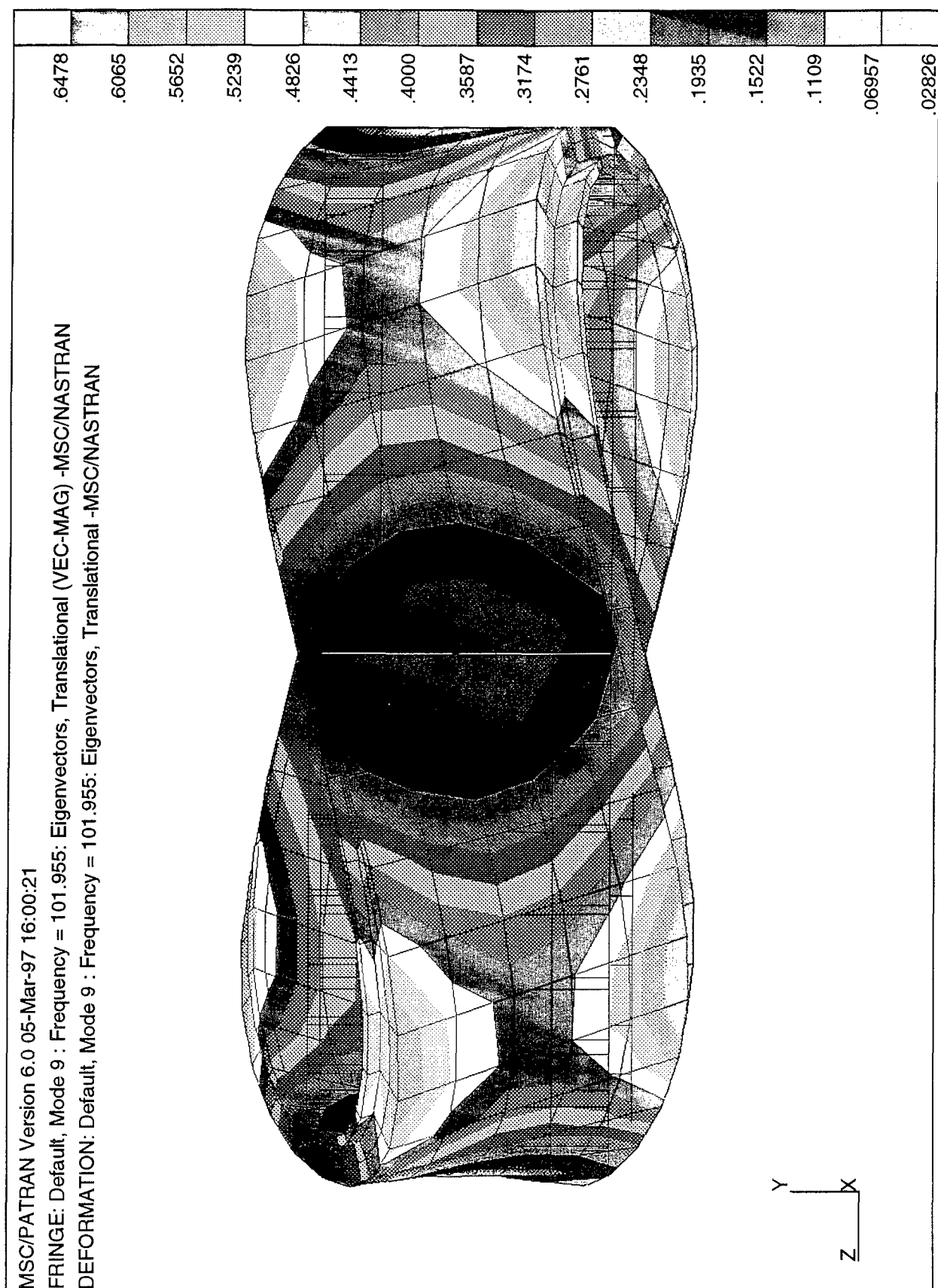


Figure 17. Mode 9, 101.96 Hz, Twisting Mode. Coil.

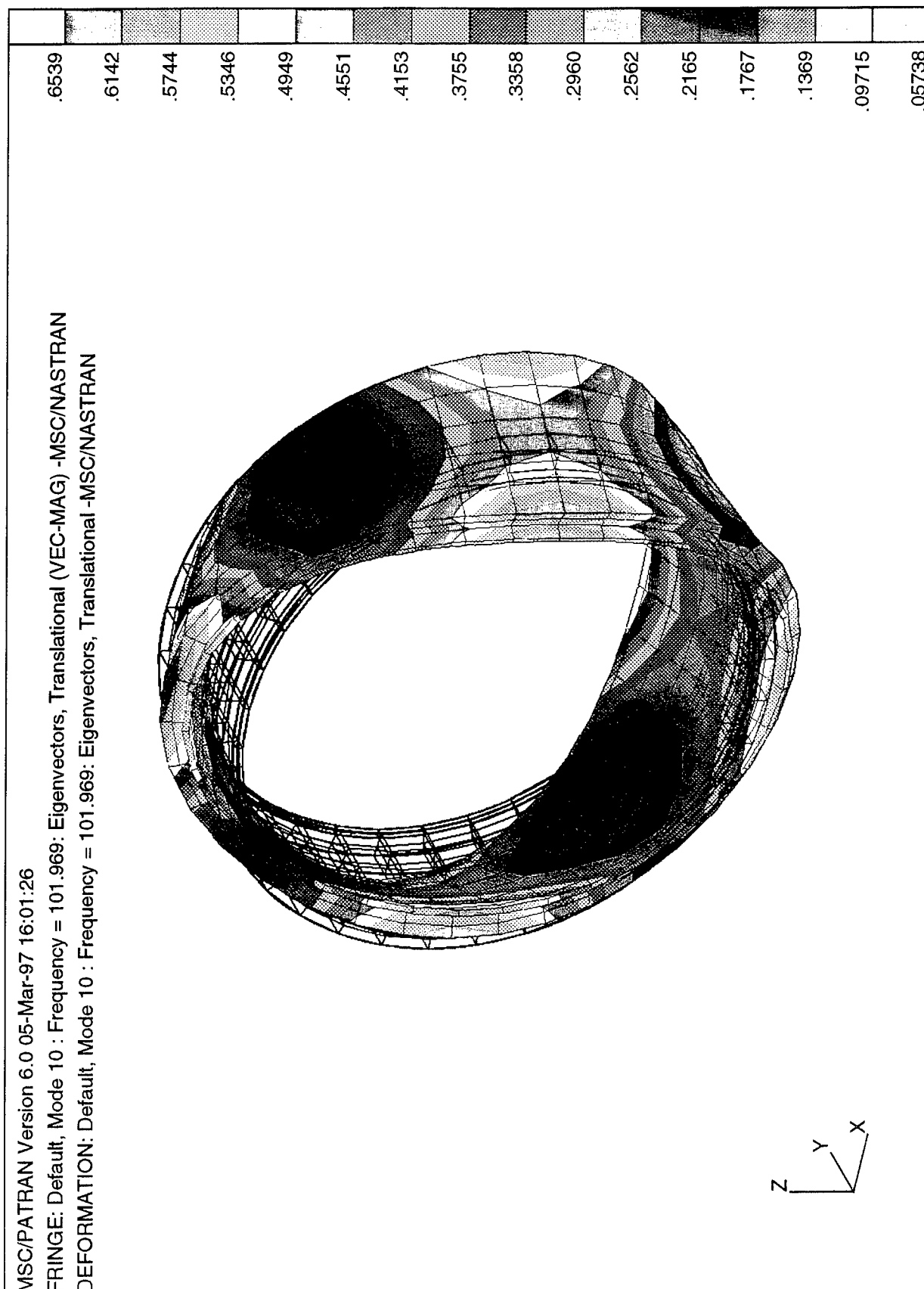


Figure 18. Mode 10, 101.97 Hz, Combined Bending Mode. Coil.

5. DISCUSSIONS

The use of small size and low power requirements of magnetic ALISS may provide significant capability in the area of magnetic mine sweeping. Due to the small size, it can be employed in a variety of platforms, including advanced design surface ships and aircraft. However, the potential advantages are offset by the risks inherent in the use of immature technologies in the unknown operational environment. Since ALISS is designed to operate while mounted to a moving vehicle, the vibration created in the system must be properly isolated within the system to ensure proper operation of the superconductor. Furthermore, ALISS is subjected to shock loads from underwater explosions (UNDEX). In this shock environment, it is possible for the superconducting magnet to become resistive. The goal of this work has been to construct a finite element model of the magnetic ALISS module, and perform the modal analysis for the purpose of providing recommendations for the shock and vibration design criteria of ALISS.

Once the normal mode analysis of the ALISS model was conducted, a transient response of the model will be analyzed using a base excitation function. For a transient input, half sine-wave acceleration with maximum amplitude and duration from ship shock detonation data can be used. It may be more realistic to consider a function of several sine waves with decaying amplitude as a transient excitation.

To understand the ALISS system and inter-relation of its components, it is also necessary to perform the sensitivity analysis by changing one property as a time. First, a damping sensitivity need to investigate by increasing the damping extant in the system. The results can be used to determine the actual structural damping when a test data obtained from the prototype is available.

Second, dimensional sensitivity must be performed by changing certain parts of the model, most notable the shell thicknesses. This will determine what effect different shell thicknesses would have on the vibration characteristics of the module.

The General Atomics is building a prototype magnetic module that will be operationally tested for shock and vibration. When the results of these tests become available, they should be compared with the data obtained from this work.

APPENDIX A. MODE SHAPES OF ALISS

The origin is located at the centroid of the magnet, the Y-axis is the bore axis of the magnet, the X-axis and Z-axis are vertical and transverse directions, respectively. "MAX" parameter used in the table is not physical dimensional value, but relative quantity and not to be scaled.

MODE 1 AND 2 FREQUENCY: 47.44 Hz

PART	MAX	DESCRIPTION
Coil/Overwrap	0.4491	
Outer S-Glass Cylinder	0.440	
Middle E-Glass Cylinder	0.3056	
inner E-Glass cylinder	0.2406	Axial, lateral translation, and rocking
Thermal Shield	0.2599	
10K Titanium Ring	0.3461	
40K Titanium Ring	0.2611	

MODE 3 FREQUENCY: 62.97 Hz

PART	MAX	DESCRIPTION
Coil/Overwrap	0.4280	
Outer S-Glass Cylinder	0.3885	
Middle E-Glass Cylinder	0.3276	
inner E-Glass cylinder	0.2169	Breeding mode in radial direction
Thermal Shield	0.3045	
10K Titanium Ring	0.3494	
40K Titanium Ring	0.2487	

MODE 4 AND 5 FREQUENCY: 64.54 Hz

PART	MAX	DESCRIPTION
Coil/Overwrap	0.6150	
Outer S-Glass Cylinder	0.5984	
Middle E-Glass Cylinder	0.4224	
inner E-Glass cylinder	0.1382	Bending mode
Thermal Shield	0.1910	
10K Titanium Ring	0.4693	
40K Titanium Ring	0.1382	

MODE 6 AND 7 FREQUENCY: 75.50 Hz

PART	MAX	DESCRIPTION
Coil/Overwrap	0.6092	
Outer S-Glass Cylinder	0.6321	
Middle E-Glass Cylinder	0.5131	
inner E-Glass cylinder	0.1770	Rocking & Bending mode
Thermal Shield	0.4148	
10K Titanium Ring	0.7100	
40K Titanium Ring	0.3321	

MODE 8 FREQUENCY: 86.15 Hz

PART	MAX	DESCRIPTION
Coil/Overwrap	0.4168	
Outer S-Glass Cylinder	0.4163	
Middle E-Glass Cylinder	0.2844	
inner E-Glass cylinder	0.1266	Axial Translation motion
Thermal Shield	0.42344	
10K Titanium Ring	0.3935	
40K Titanium Ring	0.2344	

MODE 9 FREQUENCY: 101.96 Hz

PART	MAX	DESCRIPTION
Coil/Overwrap	0.6478	
Outer S-Glass Cylinder	0.9134	
Middle E-Glass Cylinder	1.0360	
inner E-Glass cylinder	0.1189	Twisting motion
Thermal Shield	0.5535	
10K Titanium Ring	1.2060	
40K Titanium Ring	0.2061	

MODE 10 FREQUENCY: 101.97 Hz

PART	MAX	DESCRIPTION
Coil/Overwrap	0.6539	
Outer S-Glass Cylinder	0.9212	
Middle E-Glass Cylinder	1.0440	
inner E-Glass cylinder	0.1198	Combined bending mode
Thermal Shield	0.5580	
10K Titanium Ring	1.2170	
40K Titanium Ring	0.2085	

LIST OF REFERENCES

1. Golda, E. M., Walters, J. D., and Green, G. F., "Application of Superconductivity to Very Shallow Water Mine Sweeping," *Naval Engineering Journal*, May 1992, pp. 53-64.
2. Hoy, E. H., "Shock and Vibration Analysis of a Superconducting Magnet System used for Mine Countermeasures," *Thesis Naval Postgraduate School*, March 1995
3. Preliminary Design Report, "Advanced Lightweight Influence Sweep System (ALISS): Magnetic Subsystem," GA-C22221. General Atomics, San Diego, CA., September, 1995.
4. Golda, E. M. et al, CARDIVNSWC-TR-81-94/31, September 1994.
5. Joseph, J. A. (ed.), *MSC/NASTRAN Users Manual*, Vols. 1 & 2, MacNeal-Schwendler Corp., Los Angeles, CA.

INITIAL DISTRIBUTION LIST

- | | |
|---|---|
| 1. Defense Technical Information Center
Cameron Station
Alexandria, Virginia 22304-6145 | 2 |
| 2. Library, Code 52
Naval Postgraduate School
Monterey, California 93943-5002 | 2 |
| 3. Professor Y. S. Shin, Code ME/Sg
Department of Mechanical Engineering
Naval Postgraduate School
Monterey, California 93943 | 1 |
| 4. Professor M. Lee, Code ME/Lm
Department of Mechanical Engineering
Naval Postgraduate School
Monterey, California 93943 | 1 |
| 5. Dr. E. Michael Golda, Code 812
Carderock Division, Naval Surface Warfare Center
3A Leggett Circle
Annapolis, Maryland 21402-5067 | 2 |
| 6. Mr. Michael J. Superczynski, Code 812
Carderock Division, Naval Surface Warfare Center
3A Leggett Circle
Annapolis, Maryland 21402-5067 | 1 |
| 7. Mr. Edward V. Thomas, Code 812
Carderock Division, Naval Surface Warfare Center
3A Leggett Circle
Annapolis, Maryland 21402-5067 | 1 |

- | | |
|--|---|
| 8. Mr. Thomas H. Fiske, Code 812 | 1 |
| Carderock Division, Naval Surface Warfare Center | |
| 3A Leggett Circle | |
| Annapolis, Maryland 21402-5067 | |
| 9. Mr. Geoffrey F. Green, Code 812 | 1 |
| Carderock Division, Naval Surface Warfare Center | |
| 3A Leggett Circle | |
| Annapolis, Maryland 21402-5067 | |
| 10. Mr. Joseph Tannenbaum, Code 812 | 1 |
| Carderock Division, Naval Surface Warfare Center | |
| 3A Leggett Circle | |
| Annapolis, Maryland 21402-5067 | |
| 11. Mr. Mike Heiberger | 1 |
| General Atomics | |
| P.O. Box 85608 | |
| San Diego, CA 92186-9784 | |
| 12. Mr. W. P. Creedon | 1 |
| General Atomics | |
| P.O. Box 85608 | |
| San Diego, CA 92186-9784 | |